Biochimica et Biophysica Acta 1837 (2014) 1756–1768

Contents lists available at ScienceDirect

Biochimica et Biophysica Acta

journal homepage: www.elsevier.com/locate/bbabio

Excitation dynamics in Photosystem I from *Chlamydomonas reinhardtii*. Comparative studies of isolated complexes and whole cells

Wojciech Giera [a,*], Sebastian Szewczyk [a], Michael D. McConnell [b], Joris Snellenburg [c], Kevin E. Redding [b], Rienk van Grondelle [c], Krzysztof Gibasiewicz [a]

[a] Department of Physics, Adam Mickiewicz University, ul. Umultowska 85, 61-614 Poznań, Poland
[b] Department of Chemistry and Biochemistry, Arizona State University, 1711 S. Rural Rd, Box 871604, Tempe, AZ 85287-1604, USA
[c] Department of Physics and Astronomy, Vrije Universiteit, De Boelelaan 1081, 1081 HV Amsterdam, The Netherlands

ARTICLE INFO

Article history:
Received 20 January 2014
Received in revised form 15 June 2014
Accepted 18 June 2014
Available online 25 June 2014

Keywords:
Photosystem I
Light harvesting complex I
Chlamydomonas reinhardtii
Time-resolved fluorescence
Streak camera
Red chlorophylls

ABSTRACT

Identical time-resolved fluorescence measurements with ~3.5-ps resolution were performed for three types of PSI preparations from the green alga, *Chlamydomonas reinhardtii*: isolated PSI cores, isolated PSI–LHCI complexes and PSI–LHCI complexes in whole living cells. Fluorescence decay in these types of PSI preparations has been previously investigated but never under the same experimental conditions. As a result we present consistent picture of excitation dynamics in algal PSI. Temporal evolution of fluorescence spectra can be generally described by three decay components with similar lifetimes in all samples (6–8 ps, 25–30 ps, 166–314 ps). In the PSI cores, the fluorescence decay is dominated by the two fastest components (~90%), which can be assigned to excitation energy trapping in the reaction center by reversible primary charge separation. Excitation dynamics in the PSI–LHCI preparations is more complex because of the energy transfer between the LHCI antenna system and the core. The average trapping time of excitations created in the well coupled LHCI antenna system is about 12–15 ps longer than excitations formed in the PSI core antenna. Excitation dynamics in PSI–LHCI complexes in whole living cells is very similar to that observed in isolated complexes. Our data support the view that chlorophylls responsible for the long-wavelength emission are located mostly in LHCI. We also compared in detail our results with the literature data obtained for plant PSI.

1. Introduction

Naturally occurring photosynthesis is the most widespread process of converting solar light into chemical energy on our planet. In cyanobacteria, algae and plants, the light-dependent phase of photosynthesis is carried out by two types of pigment–protein complexes embedded in thylakoid membranes: Photosystem I (PSI) and Photosystem II (PSII). The main function of PSI is to catalyze light-driven electron transport from plastocyanin to ferredoxin, which are located on opposite sides of the thylakoid membrane. Most of the PSI pigments compose an antenna system that captures sunlight energy and transfers it to the reaction center (RC), where transmembrane electron transfer is initiated [1]. PSI consists of a core antenna system directly coupled to the RC and, in the case of plants and algae, additional light harvesting complexes (LHCI), which support effective collection of the light. In plants, the LHCI system is composed of four proteins labeled Lhca1–4 [2–4]. In the case of algae, the number of additional Lhca polypeptides is larger and it was estimated by different research groups to be in the range of 9–14 [5–7].

PSI core of higher plants and algae is composed of at least 14 different protein subunits and a pool of pigments: 96–103 chlorophylls *a* and about 22 carotenoid molecules identified as beta-carotene [3,8–10]. The main subunits, PsaA and PsaB, with molecular masses of 82–84 kDa, are homologous and form a heterodimer that binds most of the electron transport chain (ETC) components as well as a significant portion of the available pool of antenna pigments. The two [4Fe–4S] clusters serving as the terminal electron acceptors are bound by the 9-kDa PsaC subunit [3]. The remaining core subunits have masses of 4–18 kDa and bind the rest of the pigments, but they do not bind any of the electron transfer cofactors. These subunits also play a role in stabilizing the structure of the PSI complex, as well as binding the diffusible electron donor and acceptor proteins [3,8].

The PSI electron transport chain (ETC) is built of six chlorophylls, two quinones and three [4Fe–4S] iron–sulfur clusters. An important issue is the proper naming of the ETC cofactors identified in the crystal structure. We have adopted the scheme proposed by Redding and van der Est [11]. However, in parentheses we present the semi-traditional, pre-structural names, which are still widely used. ETC chlorophylls and quinones are associated with the protein subunits PsaA and PsaB

Abbreviations: PSI, Photosystem I; LHCI, light-harvesting complex I; Chl, chlorophyll; RC, reaction center; ETC, electron transfer chain; TR, time range; DAS, decay-associated spectrum

* Corresponding author. Tel.: +48 61 8295251.
E-mail address: w_giera@amu.edu.pl (W. Giera).

http://dx.doi.org/10.1016/j.bbabio.2014.06.004
0005-2728/

and arranged in two quasi-symmetrical branches: A and B. The beginning of both branches is a heterodimer of chlorophyll *a*, referred to as $ec1_B$ or P_B, and chlorophyll *a′*, referred to as $ec1_A$ or P_A. This heterodimer is traditionally called P700, due to the peak wavelength of its absorption. Another pair of cofactors (A and A_0) in each branch is composed of two chlorophylls *a*, labeled as $ec2_A$ and $ec3_A$ (branch A) or $ec2_B$ and $ec3_B$ (branch B). The next electron carrier in each branch is a phylloquinone molecule (A_1) denoted as PhQ_A (branch A) or PhQ_B (branch B). Both branches meet together at the [4Fe–4S] cluster called F_X, which is an interesting example of inter-polypeptide cofactor coordinated by two different protein subunits (PsaA and PsaB). The terminal electron acceptors are two additional [4Fe–4S] clusters associated with stromal subunit PsaC and denoted as F_A and F_B. Until recently, the controversial issue was the activity of each of the cofactor branches in the electron transport. It is now known that in the case of algae both paths are almost equally involved in this process [11–17].

The ETC cofactors involved directly in the primary charge separation steps, together with the protein framework, are commonly referred to as reaction center (RC). According to the classical model, the primary electron donor was P700 and the primary electron acceptor was $ec3_A$ or $ec3_B$. In the last few years, however, it was shown by two groups that the primary charge separation is a reversible process and occurs within the $ec2_A$–$ec3_A$ or $ec2_B$–$ec3_B$ pair [17–20] with $ec2_{A/B}$ and $ec3_{A/B}$ being the primary electron donor and acceptor, respectively. It should be noted, however, that there are some important differences between the model proposed by Giera and co-workers [20] and the results of Holzwarth and co-workers [19], in particular with regard to the fluorescence spectrum of the excited reaction center (RC*) and the total rate of excitation decay in the antenna system of the algal PSI core. In this article we discuss the source of these discrepancies.

Another important objective of the study presented here was to determine the excitation dynamics in isolated algal PSI–LHCI complexes and compare it with PSI–LHCI complexes working in membranes in whole living cells. Time-resolved fluorescence spectra for isolated PSI–LHCI from *Chlamydomonas reinhardtii* obtained with a streak camera have been published [21] but only for complexes with open RC and in a limited time window (~550–800 ps). Moreover, they were not compared directly with comparable data using PSI cores. Therefore we decided to carry out new measurements for the PSI–LHCI complexes, both with open and closed RC and in various time windows, to get a more complete picture of the energy transfer process in this system. In particular, one of our goals was to determine the effective time of the excitation energy transfer from LHCI antennas to the PSI core.

Whole cells of *C. reinhardtii*, genetically lacking PSII and most of the LHCII, were examined a long time ago, but with a lower temporal resolution (the instrument response function of 50–70 ps, FWHM) [22,23]. Our whole-cell measurements, carried out under the same conditions as for the isolated complexes, allowed us to compare PSI in both contexts and determine if the isolation procedure affected the observed excitation dynamics.

2. Materials and methods

The experiments were performed on three samples based on the green alga, *C. reinhardtii*: (1) isolated PSI core particles, (2) isolated PSI–LHCI complexes, (3) whole living cells. For the whole cells and isolated PSI core particle measurements, we used the CC2696 strain from the *Chlamydomonas* Culture Collection at Duke University. The CC2696 strain carries a deletion in the chloroplast *psbA* gene, causing a complete loss of Photosystem II, and also contains the DS-521 nuclear mutation leading to a 90% reduction in LHCII content and some minor modifications in the polypeptide composition of LHCI [22].

The CC2696 cells were grown heterotrophically at 25 °C in CC liquid medium [24]. The thylakoid membranes were isolated according to the method presented by Chua and co-workers [25]. The PSI core particles were extracted from thylakoid membranes by detergent (n-dodecyl-β-D-maltoside) treatment and purified by weak anion exchange chromatography, using protocols described previously by Ramesh and co-workers [26]. This purification procedure yielded PSI preparations with a Chl *a*/P700 ratio of 85–95 [26]. This ratio is very similar to that specified for the PSI core of cyanobacteria (96 Chls) and higher plants (93 Chls), based on structural studies [3,10]. While we cannot assume that the PSI preparations obtained in this way do not contain any LHCI antennas at all, the Chl/P700 ratio clearly shows that the LHCI amount is drastically reduced in this preparation in comparison with the PSI–LHCI preparation (see below).

The PSI–LHCI complexes were isolated from *C. reinhardtii* strain JVD-1B transformed with the His_6-tagged PsaA [27]. Cells of this strain were grown heterotrophically at 25 °C in well-aerated liquid TAP (Tris–acetate–phosphate) medium [28]. The thylakoid membranes were prepared as described by Fischer and co-authors [29] and then solubilized by n-dodecyl-β-D-maltoside. PSI–LHCI complexes were purified by chemical affinity chromatography using Ni-NTA (Invitrogen) column, as previously described [27]. The Chl/P700 ratio for this preparation was estimated to be 203–209 with a ratio of chlorophyll *a* to chlorophyll *b* equal to 7.5 [27]. This would mean that the PSI–LHCI complex obtained by this method contains an average of 180 chlorophyll *a* molecules.

For spectroscopic experiments, the isolated complexes were suspended in a buffer containing 50 mM Hepes (pH = 7.2), 5 mM $MgCl_2$, 12 mM $CaCl_2$, 20% glycerol (v/v), 1 mM benzamidine, 1 mM PMSF (phenyl–methyl–sulfonyl fluoride), 1 mM EDTA, and 0.03% n-dodecyl-β-D-maltoside, whereas the whole cells were suspended in CC liquid medium (see [24,26]). In the case of isolated complexes (PSI core and PSI–LHCI) the P700 was kept neutral (open RC) by addition of 20 mM sodium ascorbate and 20 μM phenazine methosulfate (PMS) or oxidized (closed RC) by addition of 3 mM $K_3Fe(CN)_6$ (potassium ferricyanide). PMS reduced by sodium ascorbate is the most popular reducing agent used to keep PSI open [20,21,30–36]. Examples of the use of ferricyanide to the chemical oxidation of P700 can also be found in the literature [20,37–40].

The time-resolved fluorescence measurements were carried out at room temperature with a streak camera setup (Laser Centrum, Vrije Universiteit, Amsterdam). The 100-fs pulses with wavelength of 800 nm were produced by a titanium:sapphire laser (Coherent, Vitesse), amplified in a regenerative amplifier (Coherent, RegA) and used to generate the second harmonic (400 nm) in a double-pass optical parametric amplifier (Coherent, OPA). The sample was excited with a repetition rate of 125 kHz by vertically polarized pulses, the energy of which was kept at a level of 0.6, 1.2 and 2.4 nJ for the PSI–LHCI complexes, PSI core and whole cells, respectively. As we checked, such energy levels are low enough to avoid the effect of annihilation.

The fluorescence was measured at a right angle with respect to the excitation beam, resolved spectrally by a spectrograph (Chromex 250IS) and temporally by a streak camera (Hamamatsu C5680), and finally detected by a CCD camera (Hamamatasu C4880). The fluorescence signal was recorded in the synchroscan mode (period $T \approx 13$ ns) in three time ranges (TR): ~150 ps (TR1), ~350 ps (TR2) and ~1500 ps (TR3). The temporal width of the detection system response function (FWHM) was equal to ~3.5 ps in TR1, ~6 ps in TR2 and ~16 ps in TR3. The exposure times per image were 10–20 min for TR1, 5–10 min for TR2 and 2.5–5 min for TR3. Four images were averaged for each TR in order to improve the signal to noise ratio. During the experiment, the sample was placed in a rotating cuvette to ensure that each laser pulse illuminated a fully relaxed sample.

The detected streak images were analyzed globally from 630 to 775 nm with ~2.2-nm resolution using the GLOTARAN software [41]. The observed fluorescence kinetics in general depends on both the excitation wavelength λ_{exc} and detection wavelength λ_i, and can be described

by the sum of several components with an exponential time evolution [42]:

$$I(\lambda_{exc}, \lambda_i, t) = \sum_{j=1}^{n} A_j(\lambda_{exc}, \lambda_i) \cdot \exp\left(-t/\tau_j\right). \quad (1)$$

Each component is characterized by a decay time τ_j and pre-exponential factor A_j (λ_{exc}, λ_i) commonly referred to as *amplitude*. The purpose of the global analysis is to obtain a single set of parameters describing the time evolution of the signal for all analyzed detection wavelengths λ_i [42]:

$$\tau_j(\lambda_1) = \tau_j(\lambda_2) = \ldots = \tau_j(\lambda_{i-1}) = \tau_j(\lambda_i). \quad (2)$$

Then, each of the decay components obtained from the global analysis is described by the decay time τ_j and the spectral distribution of the amplitude A_j (λ_{exc}, λ_i), which is commonly called the *decay-associated spectrum* (DAS).

The global analysis of results from TR2 and TR3 was carried out together with the results from the shorter time ranges: TR2 with TR1 (TR1/2), TR3 with TR1 and TR2 (TR1/2/3). It means that they were given together as input data and fitted simultaneously to obtain the same set of DAS and decay times. Such procedure allowed us to examine the excitation dynamics at longer time windows and maintain, at the same time, a good temporal resolution characteristic for shorter time ranges (see above). Components with decay times much longer than experimental time windows were fitted using the *back sweep* signal, i.e. fluorescence that remains after the half of the synchroscan period T and is overwritten on the initial fluorescence decay. It was estimated that standard errors for decay times did not exceed 2.5% of the decay times' values.

Decay times obtained from the global analysis may be very often associated directly with the lifetimes of different states occurring in the investigated sample. Obviously these lifetimes describe only the overall time evolution of those states and are not the inverse of the real rates of the forward and backward transitions between them. Such rate constants are not measurable directly and can be obtained only by fitting the specific kinetic model to the data (in the fitting procedure called target analysis). In this work, description of the results will be limited only to the lifetimes obtained directly in the global analysis.

The fractional contribution of each component to the total fluorescence decay α_j and the average excitation lifetime $\langle\tau\rangle$ were calculated based on the TR1/2/3 data according to the equations

$$\alpha_j = \left(I_j / \sum_{j=1}^{n} I_j\right) \cdot 100\% \quad (3)$$

and

$$\langle\tau\rangle = \sum_{j=1}^{n} \left(I_j \cdot \tau_j\right) \Big/ \sum_{j=1}^{n} I_j, \quad (4)$$

where I_j is the integrated area of individual DAS.

3. Results

3.1. PSI core

The results of global analysis for a PSI core with the RC in either the open or closed state are presented in Fig. 1. The analysis carried out only for TR1 revealed the existence of three components, whereas a combined fit of TR1 and TR2 (called TR1/2) or TR1, TR2 and TR3 (called TR1/2/3) indicated the existence of four components of fluorescence decay. The overall excitation dynamics is dominated by the two fastest components that together account for 90.6% of the total fluorescence decay in PS core preparation (TR1/2/3, Table 1) and are attributed to excitation energy trapping in the RC [19,20]. The decay times and amplitudes of the two fastest components obtained for TR1 and TR1/2/3 are virtually identical for both data sets. There are, however, some differences between the data for PSI with open and closed RC. First, the fastest component in PSI core with open RC has a decay time of ~8.5 ps, compared to ~11 ps in PSI with closed RC. Second, the ratio of the faster and slower components' contributions to the total fluorescence decay is equal to ~2 for PSI core with open RC and only ~1.3 for PSI core with closed RC (TR1/2/3, Table 1). Consequently, closing of the RC leads to a slight but noticeable slowing of fluorescence decay in PSI core, in line with previous findings [20].

The two fastest components obtained for the PSI core, both in the open and closed states, differ from one another in the long-wavelength region of spectrum, i.e. at about and above 700 nm (Fig. 1A, D, C, F). Emission in this region results mainly from strong excitonic coupling between two or more chlorophylls [1,43]. The slower (25–27 ps) component clearly has a higher contribution of this long-wavelength emission than the fastest one (~8–12 ps). One may assume that 25–27-ps DAS describes a decay of excited states equilibrated over two pools of chlorophylls: (1) the dominant pool of short-wavelength (bulk) chlorophylls emitting mainly at ~685 nm (the same as observed in the fastest component) and (2) a smaller pool of long-wavelength chlorophylls, red-shifted compared to the bulk chlorophylls and emitting mainly at about and above 700 nm. Recently a similar finding was reported for a red-chlorophyll-free Photosystem I particle isolated from *Synechococcus* WH 7803 [44]. Closing the RC changes the contributions of these two pools: only the short-wavelength emission increases, whereas the signal from the long-wavelength chlorophylls remains at a similar level.

A third component, not resolved in TR1, with a decay time of 64–84 ps for the TR1/2 fit and 290–314 ps for the TR1/2/3 fit, has a very small amplitude. Its contribution to the total fluorescence decay in TR1/2/3, calculated on the basis of DAS integrated area, is only ~3.7% (see Table 1). This contribution is even smaller (only ~2%), when the calculations are done on the basis of the amplitude value in the DAS maximum (~680 nm). This long-lived signal probably comes from small amount of free LHCI proteins contaminating the PSI core preparation (more details in the Discussion section).

The slowest component (decay time of 3.8–5.1 ns; Fig. 1) has a ~6% (TR1/2/3, see Table 1) contribution to the total fluorescence decay and its DAS maximum is blue-shifted (at 675 nm) relative to the maxima of the other components' spectra (at 685 nm). Such blue-shifted and long-lived fluorescence is characteristic of uncoupled chlorophylls, i.e. chlorophylls that are not properly connected to the rest of the antenna system and do not transfer excitation energy to RC. However, this component may also partially reflect some excitation decay in the free LHCI proteins. Thus, fluorescence of uncoupled chlorophylls and free LHCI together represents ~10% of the total signal.

In the case of global analysis for TR1/2, the decay times of all components, with the exception of the longest one, are shorter than those obtained for TR1 and TR1/2/3 but comparable to those published previously for PSI core measured in TR1/2 [20]. Such variation of the decay time values obtained for the different time windows is a consequence of the limits of global analysis. This method leads to description of experimental data by a limited number of components, each characterized by the decay time and DAS (see the Materials and methods section). None of these parameters are independent, i.e. changing one of them causes changes of the others. The longest component (3.5–5 ns) is characterized by decay times much longer than experimental time windows. However, they do not depend strongly on the experimental time window because their fits are based on the *back sweep* signal (see the Materials and methods section). Decay time of the third component, in turn, strongly depends on the analyzed time window (compare TR1/2 and TR1/2/3; Fig. 1B, E, C, F). In the case of our measurements, its value is almost always truncated to about 20–25% of the analyzed

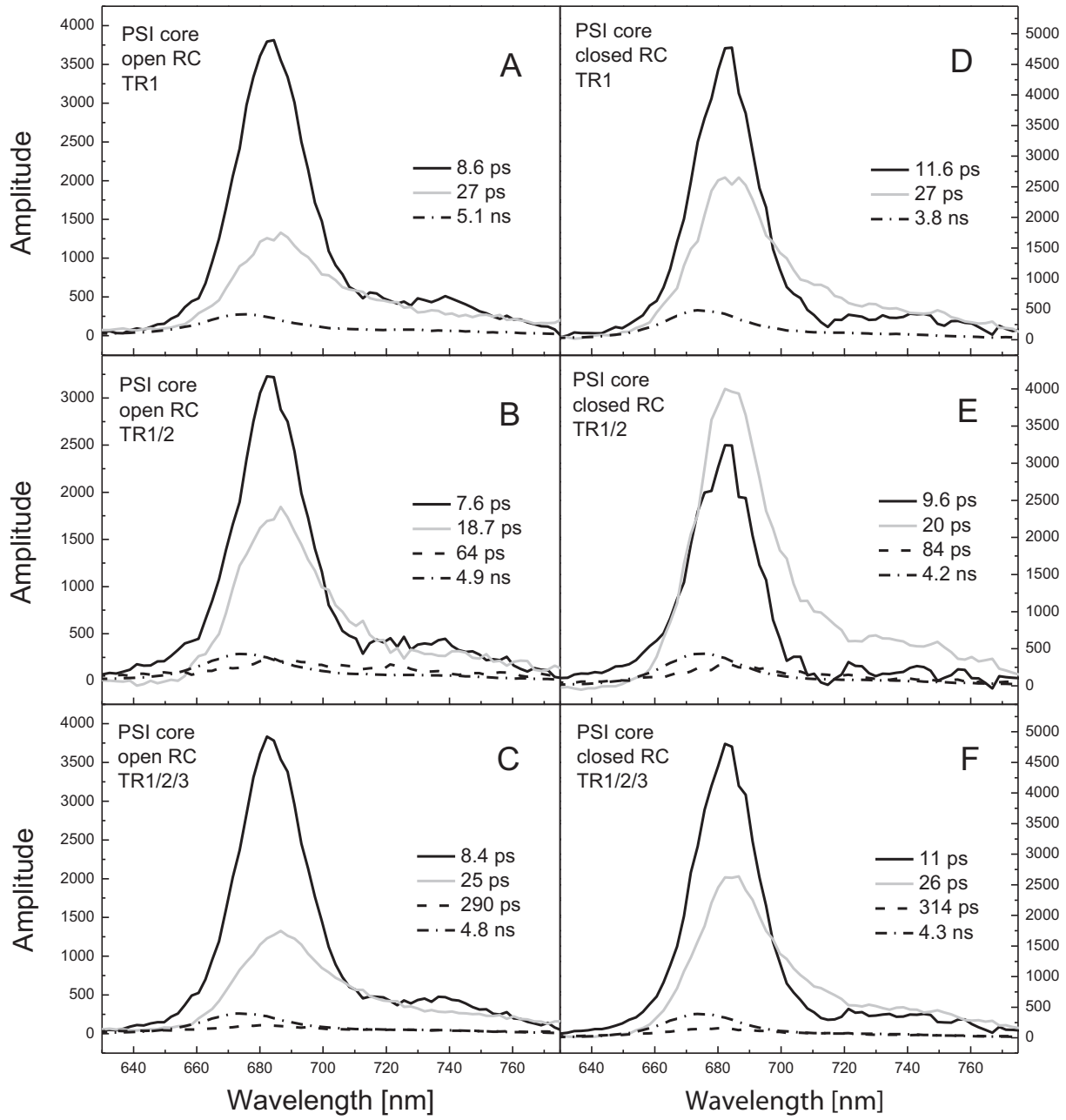

Fig. 1. Fluorescence decay associated spectra of PSI core particles from *C. reinhardtii* with RC in open state (A, B, C) and closed state (D, E, F) obtained by global analysis carried out for single TR1 data set (A, D) and simultaneously for TR1 and TR2 data sets (B, E) or for TR1, TR2 and TR3 data sets (C, F).

time window. Decay time of the third component is not an independent parameter and therefore affects the decay times of the shorter components. In the TR1/2 analysis this effect is especially strong, because the decay time of the third component (60–100 ps) is of the same order of magnitude as the decay time of the second component (~20 ps). Consequently, we also observed a shortening of the decay times of the two

Table 1
The percentage contribution of particular components to the total fluorescence decay (obtained by global analysis of TR1/2/3 data) and average excitation decay times.

PSI core				PSI–LHCI				Whole cells	
Open RC		Closed RC		Open RC		Closed RC			
8.4 ps	60.9%	11 ps	51.6%	7.7 ps	30.4%	7.6 ps	19.1%	6.6 ps	19.2%
25 ps	29.7%	26 ps	38.8%	28 ps	49.4%	30 ps	56.4%	28 ps	70.1%
290 ps	3.7%	314 ps	3.7%	274 ps	8.8%	273 ps	9.6%	166 ps	10.0%
4.8 ns	5.7%	4.3 ns	5.9%	4.3 ns	11,4%	3.5 ns	14,9%	10 ns	0,7%
$\langle\tau_{12}\rangle = 13.8$ ps		$\langle\tau_{12}\rangle = 17.4$ ps		$\langle\tau_{12}\rangle = 20.3$ ps		$\langle\tau_{12}\rangle = 24.3$ ps		$\langle\tau_{12}\rangle = 23.4$ ps	
$\langle\tau_{123}\rangle = 24.6$ ps		$\langle\tau_{123}\rangle = 29.0$ ps		$\langle\tau_{123}\rangle = 45.4$ ps		$\langle\tau_{123}\rangle = 52.5$ ps		$\langle\tau_{123}\rangle = 37.8$ ps	

$\langle\tau_{12}\rangle$ — calculated on the basis of the two fastest components, $\langle\tau_{123}\rangle$ — calculated on the basis of the three fastest components. See text for more details.

fastest components and change in the relative ratio of their amplitudes. This example shows that global analysis performed in different time windows may give different fitting results, which could unreasonably lead to different conclusions, while, in fact, they are still consistent with each other. Almost identical decay times of the two fastest components obtained for TR1 and TR1/2/3 suggest that truncation of the third component in the analysis of TR1/2/3 data has a negligible impact on the faster components. This can be explained by the long decay time of the third component (~270–300 ps) compared to the decay times of the faster components (~8–11 ps and ~25–26 ps). Therefore we will base our conclusions mainly on the fits obtained for TR1/2/3.

In summary, the excitation dynamics in our PSI core preparation is dominated by biphasic trapping of the bulk chlorophyll excited states, accompanied by two additional processes: (1) a decay of excited states of long-wavelength chlorophylls with a lifetime of ~26 ps and (2) a slow decay of excited states of uncoupled chlorophylls or chlorophylls attached to some very small fraction of free LHCI present in the sample.

3.2. PSI–LHCI

The results of global analysis for the PSI–LHCI complexes with the RC in open or closed state are presented in Fig. 2. The analysis of the data obtained in TR1 revealed the existence of three components. The amplitudes of the two fastest components (decay times of 8 and 31 ps in open state) peak at about 685 nm, whereas the amplitude of the longest-lived component (decay time of 3.8 ns in open state) has a maximum at about 680 nm and is much larger than the corresponding component in the PSI core preparation.

When comparing the TR1 data for PSI core and PSI–LHCI complexes in open states one can see three major differences (Fig. 1A and 2A). First,

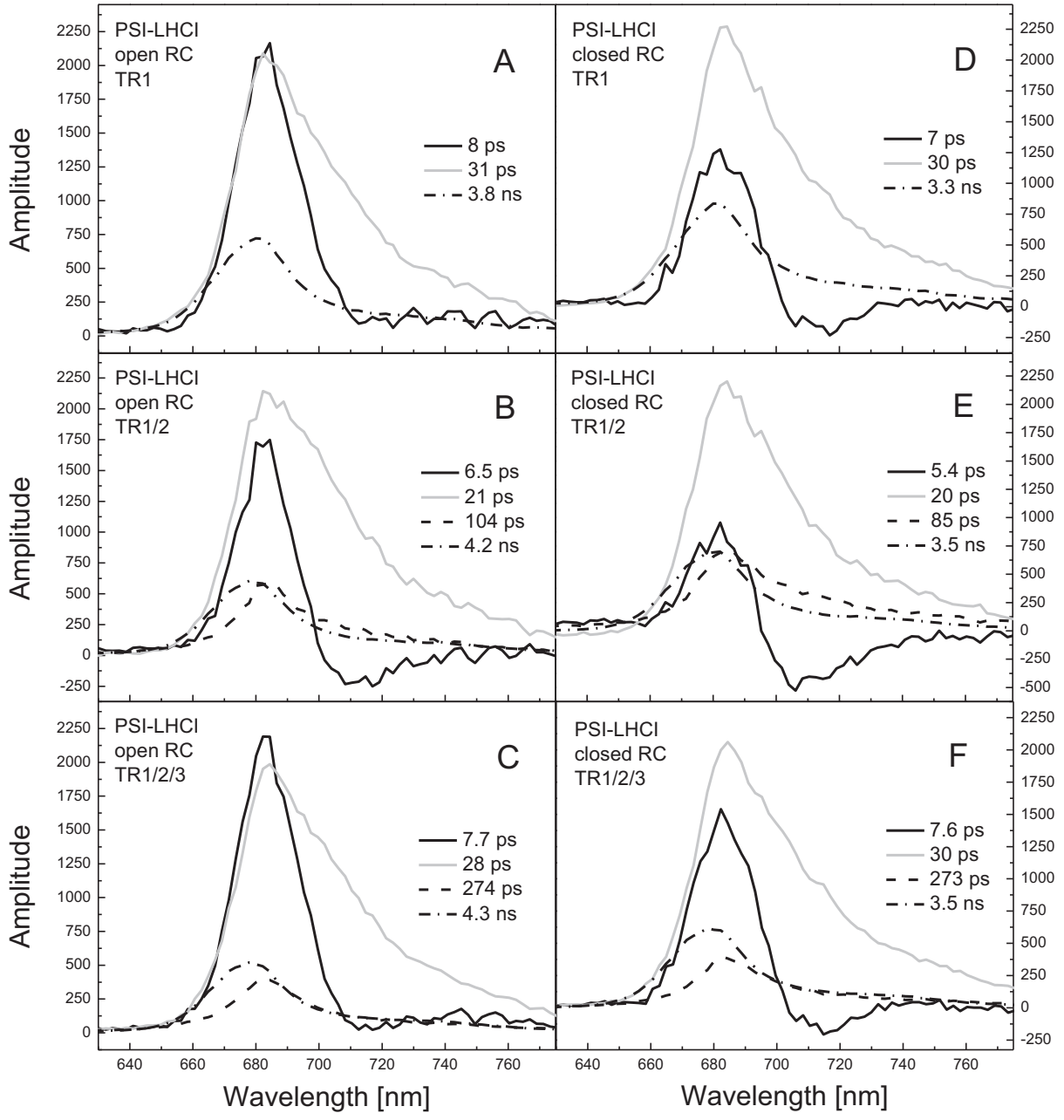

Fig. 2. Fluorescence decay associated spectra of PSI–LHCI complexes from *C. reinhardtii* with RC in open state (A, B, C) and closed state (D, E, F) obtained by global analysis carried out for a single TR1 data set (A, D) and simultaneously for TR1 and TR2 data sets (B, E) or for TR1, TR2 and TR3 data sets (C, F).

the amplitudes of the two fastest components in PSI–LHCI complexes are of similar size at the maximum, in contrast to the PSI core. Second, the decay time of the second component (31 ps) is ~4 ps longer than the decay time of the analogous component in the PSI core. Third, the long-wavelength tail in the 31-ps DAS is clearly more pronounced than that in the corresponding DAS obtained for PSI core. In consequence, the contribution of the 31-ps component to the total excitation decay in PSI–LHCI complexes is bigger than the contribution of the fastest component.

Closing the RC leads to changes in amplitude ratios and spectral distributions. The amplitude of the 7-ps component becomes much lower at 685 nm compared to the 30-ps component and is characterized by negative values above 695 nm. This means that above 695 nm this component describes a fluorescence *rise* with a characteristic time of 7 ps. Fluorescence decay in one spectral region accompanied by similar fluorescence rise (with similar lifetime and absolute integrated area of the DAS) in another spectral region is characteristic of excitation energy equilibration between two spectrally different pools of chlorophylls. It should be noted here that I_j in Eqs. (3) and (4) is obtained by mathematical integration of individual DAS in the entire analyzed spectral window, i.e. it is a difference between absolute area under the positive part of the DAS and absolute area under the negative part of the DAS. Thus, in our calculations the excitation equilibration process gives no net contribution to the total fluorescence decay (see below).

Combined analysis of TR1/2/3 gives four components of fluorescence decay (Fig. 2, Table 1). The two fastest components have decay times, amplitudes sizes and shapes similar to those obtained for TR1. An additional component with a decay time of 273–274 ps has a quite significant contribution to the total fluorescence decay (~9%, see Table 1), in contrast to the PSI core, and peaks at about 683 nm. The long-lived component (3.5–4.3 ns) has a maximum at about 678 nm. The spectral shape of the two longest components in TR1/2/3 suggests that in TR1 they were replaced by one long-lived component with amplitude maximum at about 680 nm and a decay time of 3.3/3.8 ns.

In the case of global analysis for TR1/2 we observed shortening of the decay times of all components (with the exception of the long-lived one). This effect has been already described in detail for the PSI core data (see above). The fastest component's contribution to the fluorescence decay around 683 nm is even lower than in the fit of TR1 or TR1/2/3. In turn, the negative part of this component above 695 nm is now much bigger. These observations agree well with those obtained by Ihalainen and co-workers for PSI–LHCI complexes measured in a slightly longer time window (~550–800 ps) [21]. In the case of closed RCs, the areas under the positive and negative parts of this spectrum are almost identical. Such characteristic conservative shape of the amplitude indicates that this component describes now almost exclusively the excitation energy equilibration between two spectrally different pools of chlorophylls.

When comparing the global analysis results for different time windows and different states of RCs (open and closed), one can find that the process of excitation energy equilibration in the particular cases is not equally represented in the fastest component's DAS. Purely conservative DAS, which could be assigned to this process, is observed only in the case of PSI–LHCI with closed RC measured in TR1/2 (Fig. 2E). The negative values of DAS above 695 nm, describing fluorescence rise in this spectral region, are also observed in the case of PSI–LHCI with open RC measured in TR1/2 (Fig. 2B) and in the case of PSI–LHCI with closed RC measured in TR1 (Fig. 2D) and TR1/2/3 (Fig. 2F), but the shape of DAS is not conservative, i.e. positive part of DAS below 695 nm is dominant. In the case of PSI–LHCI with open RC measured in TR1 (Fig. 2A) and TR1/2/3 (Fig. 2C) we do not observe negative DAS at all. However, the observed variation is not the effect of different efficiencies of excitation equilibration in particular cases but rather results from the limits of the performed analysis. Processes of excitation decay due to trapping and excitation equilibration occur in the PSI samples with the similar lifetimes. Thus, their separate detection is problematic, because the same component must describe both processes and its total DAS is a sum of positive DAS characteristic for the first process and conservative DAS of the second process. The situation is even more complicated, because particular decay components, obtained for different conditions of analysis, may reflect different combinations of processes occurring in the sample. Therefore, some processes may be more easily detected in one analysis condition than in the others. Purely conservative DAS was observed only in the case of PSI–LHCI with closed RC measured in TR1/2. Its decay time is equal to 5.4 ps and is shorter than the decay times of analogous components in the rest of fitted data (7–8 ps). This may suggest that the excitation energy equilibration is slightly faster than the first, fast phase of trapping. Consequently, when we fit both processes with one component, they give different contributions to the total DAS of the fastest component, dependent on the fitted decay time. Closing of RC leads to a slowdown of the energy trapping and then the excitation equilibration process is also much better represented in the fastest component. In the case of PSI core (see above), the amount of excitations transferred to long-wavelength chlorophylls is so low, that even the closing of the RC or shortening of the decay times in TR1/2 does not improve our observation of the excitation energy equilibration.

3.3. PSI core vs. PSI–LHCI

As shown and discussed above, the fluorescence decay in both the PSI core and PSI–LHCI can be generally described by three decay times: 7–8 ps, 25–30 ps and 273–314 ps (the exception is the PSI core with closed RC, for which the shortest decay time is ~11 ps). However, these three components in the two preparations have different amplitude sizes and spectral shapes. Therefore, for better interpretation of the data, we decided to perform a simultaneous analysis of the fluorescence decays measured in TR1 for PSI core and PSI–LHCI (with open RC); i.e. they were taken together as input data in a single global analysis. We attempted to fit the identical fluorescence decay times for both preparations, assuming that the spectral distribution of analogous components could be different between the PSI core and PSI–LHCI. Decay associated spectra obtained in this way are shown in Fig. 3. An additional component with decay time of 161 ps was found, which was impossible to resolve in the global analysis of single TR1 data set, probably due to the limited time window (~150 ps).

The most striking difference between the PSI core and the PSI–LHCI complex is the spectral shape of the fastest component. In the case of PSI–LHCI complexes, this component describes almost exclusively the excitation energy equilibration between short- and long-wavelength chlorophylls, whereas in the PSI core this component describes only fluorescence decay without any signal rise above 695 nm. Moreover, the 17-ps component spectrum is much more pronounced above 695 nm for PSI–LHCI than it is for the PSI core. Another clear difference between the two samples is the much larger amplitude of the 161-ps component in PSI–LHCI, compared to the analogous component in the PSI core. As one can see, the simultaneous global analysis of two different preparations allowed us to extract clearly two important processes occurring in PSI–LHCI complexes, initially irresolvable in a single analysis of the TR1 data: energy equilibration between short- and long-wavelength chlorophylls and a much slower decay (~160 ps) of a significant part of the excitations.

One can raise the question of the correctness of such simultaneous analysis. However, we should always keep in mind that global analysis is only the kind of mathematical description of the experimental data by some limited number of parameters. In the typical global analysis (single data set obtained for one sample) the same lifetimes are fitted for different detection wavelengths. Thus, we could also ask whether this standard approach is correct. What defines the correctness of the fitting results? In our opinion, we should not discuss the correctness of the fit, but rather its quality, which can be controlled by a specific numeric parameter, like chi square or root mean square (RMS). Generally,

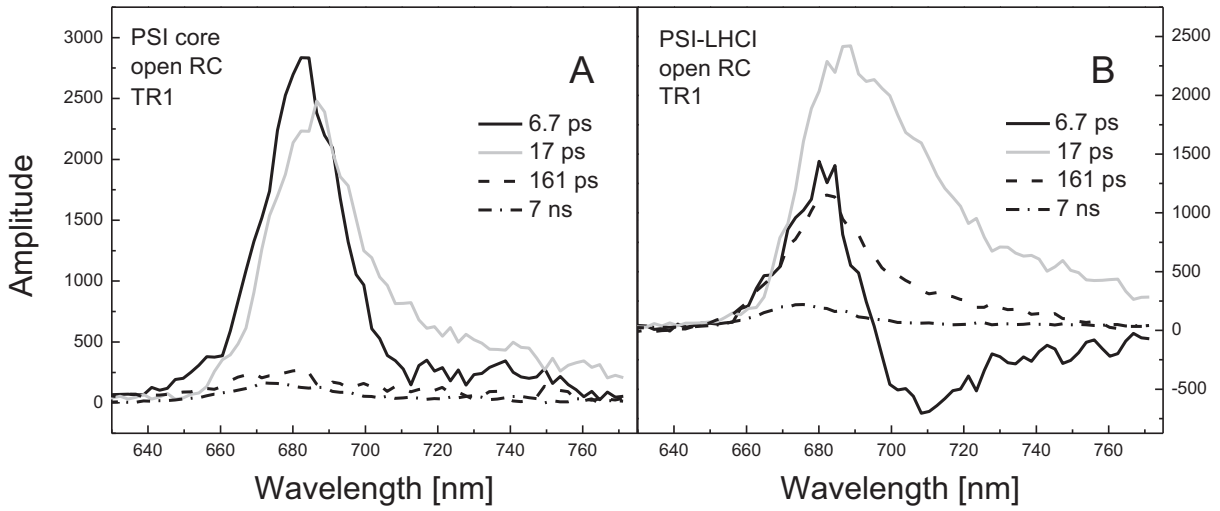

Fig. 3. Fluorescence decay associated spectra obtained by simultaneous global analysis of the fluorescence decays measured in TR1 for PSI core particles and PSI–LHCI complexes (with open RC). The identical fluorescence lifetimes were fitted for both preparations with the assumption that the spectral distribution of analogous components could be different for PSI core (A) and PSI–LHCI (B).

we can fit the same data set using different combinations of decay-times and pre-exponential factors (amplitudes/DAS) and these fits will differ from one another in quality. Of course, there is a question of what quality can be treated as acceptable. This choice is of course arbitrary. However, it is also possible that two different sets of fitting parameters describe the experimental data with very similar or almost equal quality. Then both fitting results are acceptable, but during interpretation we need to remember that particular decay components obtained in these two fits reflect different combinations of processes occurring in the sample. The quality (residuals and RMS parameter) of the simultaneous fit of PSI core and PSI–LHCI presented here was comparable with the quality of the single fits (data not shown).

3.4. Whole cells

Global analysis of fluorescence decay in whole cells (Fig. 4) shows that dynamics of most of excitations (~90%) in PSI–LHCI complexes in vivo can be described by two components similar to those observed in vitro for PSI–LHCI complexes with closed RC (Fig. 2). Therefore it seems that most of the PSI RCs in whole cells remain closed during the experiment. In the case of whole living cells, it is not possible to chemically control the redox state of P700 and therefore $P700^+$, produced due to charge separation, can be re-reduced to P700 only in the natural way, i.e. by electron transfer from plastocyanin. Generally, under a single-turnover excitation, the kinetics of $P700^+$ reduction by reduced plastocyanin (both in vitro and in vivo) can be described by two components with lifetimes of 5–10 μs and 60–140 μs [45–47]. In the whole cells of *C. reinhardtii* (including those deficient in PSII) the first phase is dominant [12,15,45,48]. In our experiment, the interval between two consecutive laser pulses was about 8 μs (repetition rate of laser: 125 kHz), that is comparable with the probable lifetime of $P700^+$ re-reduction. Of course, during the streak camera experiments, all samples were placed in a rotating cuvette to ensure that each laser pulse illuminated a fully relaxed sample. However, in the case of whole cell measurements, the rotation speed had to be reduced to a minimum to avoid centrifugation and then distance traveled by the sample between two consecutive laser pulses was smaller than the diameter of the laser beam. This may have led to accumulation of $P700^+$ in the sample and, consequently, RCs in the majority of excited PSI complexes were remaining closed during the experiment.

Apart from the similarities mentioned above, we can also find two significant differences in the excitation dynamics in PSI–LHCI complexes in vitro and in vivo. First, in the whole cells the blue-shifted nanosecond component, characteristic of the uncoupled chlorophylls, practically does not exist. Secondly, the third component of fluorescence decay in whole cells is characterized by a decay time that is shorter than the analogous one in the isolated PSI–LHCI complexes (~170 ps vs ~270 ps).

4. Discussion

4.1. Reversibility of initial charge separation and the origin of red emission

The biphasic kinetics of excitation energy trapping observed for PSI core can be explained by the reversibility of primary charge separation [18–20]. The whole process can be then described as follows:

$$(\mathrm{Ant/RC})^* \rightleftarrows \mathrm{S1} \rightarrow \mathrm{S2}.$$

The emitting excited state (Ant/RC)* decays due to the charge separation process and formation of a non-emitting charge-separated state (S1), which can evolve into a secondary non-emitting state (S2). However, in this model the back reaction leading to regeneration of the excited state from S1 is not insignificant. Thus, the faster phase of fluorescence decay can be ascribed to the formation of equilibrium between the excited state and the first charge-separated state, whereas the slower phase represents decay of this equilibrium due to the secondary electron transfer step. Naturally, the decay rates of these components are not the same as the rate constants in the model presented above. It is also important to note that energy equilibration processes within the (Ant/RC)* state take place and occur at the same time-scale as energy trapping in RC (see the Results section).

It has been recently demonstrated that P700 is not the primary electron donor and that charge separation occurs rather between $ec2_A$ and $ec3_A$ or between $ec2_B$ and $ec3_B$ [17–20]. Moreover, the equilibrium between (Ant/RC)* and S1 is very sensitive to changes in the environment, e.g. the positive charge on P700 or mutations near ec3 [17,20]. Also in the PSI core measurements described here, fluorescence decay was slowed after closing of RC, which can be explained by a shift in the (Ant/RC)* ⇆ S1 equilibrium towards the excited state. A more detailed description of this phenomenon can be found in our previous article [20].

Although our model and the model proposed by Holzwarth's group [19] are apparently similar regarding the excitation dynamics in the PSI core, there are some significant differences between our experimental data and theirs. First of all, the spectral shape and amplitude ratio of

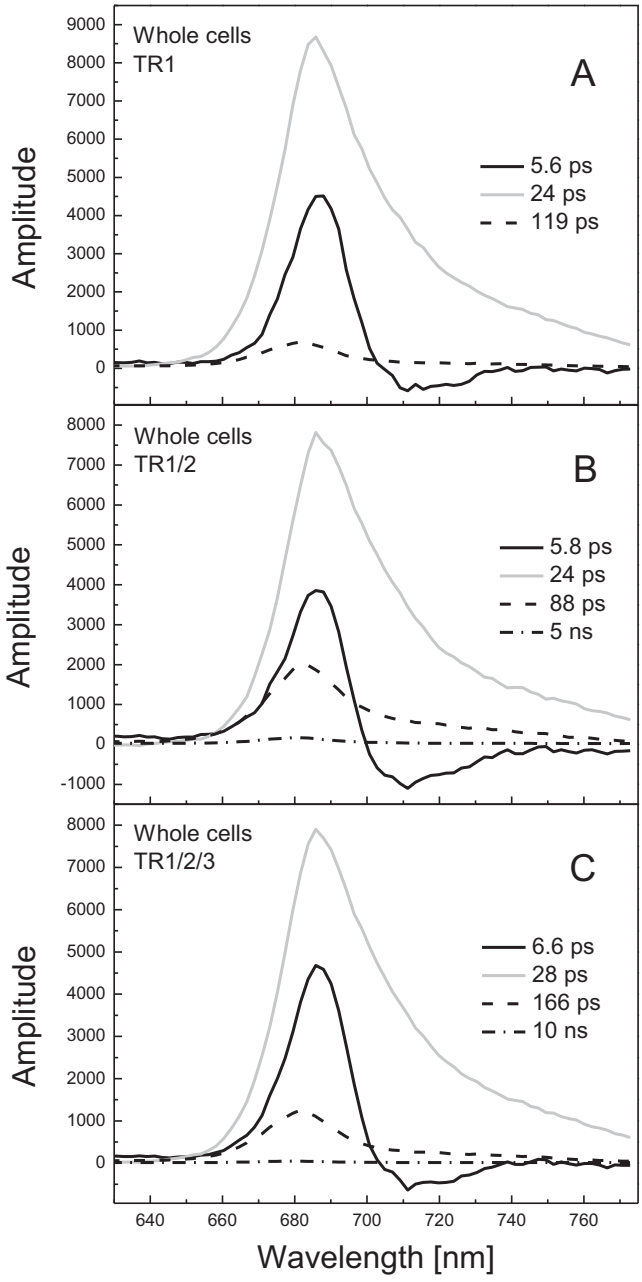

Fig. 4. Fluorescence decay associated spectra of *C. reinhardtii* whole living cells (genetically lacking PSII and most of the LHCII) obtained by global analysis carried out for single TR1 data set (A) and simultaneously for TR1 and TR2 data sets (B) or for TR1, TR2 and TR3 data sets (C).

the 8-ps and 22-ps components obtained by Holzwarth and co-workers for their PSI particles [19] are similar to those observed by us for PSI–LHCI complexes (Fig. 2B). This may suggest that they measured PSI–LHCI complexes rather than PSI core or, at least, that their PSI core was much more contaminated with LHCI antennas then ours. The second issue is that Holzwarth and co-workers disregarded the possibility of long-wavelength chlorophylls in the antenna system and assigned the whole long-wavelength signal to the excited state of reaction center (RC*). In their modeling, the RC* state is characterized by a spectrum with positive values above 690 nm and a maximum at ~715 nm. However, the long-wavelength emission was already observed not only in the whole PSI–LHCI complexes from *C. reinhardtii* [6,49] but also in the individual LHCI monomers, especially in the Lhca2, Lhca4 and Lhca9 complexes [50]. This means that the long-wavelength emission in the PSI–LHCI complexes originates, at least partially, from the long-wavelength LHCI antenna chlorophylls. Therefore, it seems very doubtful that a strong long-wavelength fluorescence observed by Holzwarth and co-workers [19] comes exclusively from the RC*.

In the case of the measurements presented here, the energy equilibration between short-wavelength (bulk) and long-wavelength chlorophylls occurs with a lifetime of ~6 ps in the PSI–LHCI complexes (Fig. 2E, 3B), but it is not clearly resolved for the PSI core preparation. The decay of excited states of long-wavelength chlorophylls is observed in both preparations and characterized generally by the ~25–30 ps lifetime (Fig. 1, 2), however it is more pronounced in the case of PSI–LHCI complexes. In the case of PSI core, the long-wavelength emission may come from the long-wavelength chlorophylls located in the RC [19,51,52] or in the core antenna [23,49,53]; neither possibility can be definitively excluded based on the present data.

4.2. Origin of the slow fluorescence decay

In addition to the two fast components discussed above, the slow excitation decay was observed in all investigated samples. In the isolated complexes it is characterized by the decay time of 275–315 ps and has an ~4% and an ~9% contribution to the overall fluorescence signal in the case of PSI core and PSI–LHCI preparations, respectively. In the case of whole cells, the analogous component represents ~10% of the total fluorescence decay, however, it has a decay time (~160 ps) shorter than that observed for isolated complexes.

A similar "extra" phase of excitation decay has been already observed in studies of PSI–LHCI complexes from algae [21,54] and plants [21,55], but its lifetime was found to be shorter than in our studies (i.e. in the range of 60–100 ps). In the case of plants, this component is clearly red-shifted, compared to the fastest ones, and describes mainly the decay of long-wavelength excitations. Its long decay time can be explained by the need for uphill excitation energy transfer from the long-wavelength chlorophylls to the bulk pool before a trapping (more details below in the section entitled Algal PSI vs. plant PSI). Our measurements as well as the previous studies [21] clearly showed that, in the case of algae, this component is not red-shifted compared to the faster one (decay time of ~25–30 ps). Therefore, there is no reason to suggest that in algae the long lifetime of this phase is the result of an uphill energy transfer from the more red-shifted forms. Thus, if the spectral properties of chlorophylls are not responsible for the slow excitation decay, we can suppose that this is an effect of some structural arrangements, which we discussed below separately for the isolated complexes and for the whole cells.

In the case of isolated PSI–LHCI preparation, the third, extra phase has much bigger contribution to the overall fluorescence decay than in the case of PSI core preparation. Thus, we can conclude that the structural effect mentioned above occurs in the LHCI antenna system and may be connected somehow with the binding between LHCI monomers and the complex. We should consider two possibilities: (1) free LHCI monomers, not attached to the PSI complexes, are present in the investigated preparations or (2) some of LHCI monomers are weakly bound to the rest of antenna system.

We rather believe that in the case of isolated complexes the first possibility takes place and the third component of fluorescence decay originates mainly from the free LHCI peptides. It was found previously that excitation decay in the reconstituted plant Lhca1–4 proteins (proteins forming the LHCI antenna system in plants) is dominated by two components with decay times of 0.7–1.6 ns and 3.1–3.6 ns [56]. The decay times observed in our measurements are shorter than those obtained even for faster phase in Lhca protein. However, this difference may result from the truncation effect, i.e. decay times of 270–310 ps are maximum values which can be fitted precisely in the time window analyzed in our experiments (more in the Results section). Moreover, the 270–310-ps component is always accompanied by the component

with lifetime of 3.5–5 ns, which can describe not only the fluorescence of uncoupled chlorophylls but also free LHCI monomers.

The second possibility, however, should be also discussed here, as it has already been proposed in the literature. Melkozernov and co-workers suggested that the observed slow excitation decay process is caused by a diffusion-limited step in the energy transfer pathway from the LHCI antenna system to the PSI core, resulting from the presence of some LHCI polypeptides only loosely bound to the rest of the LHCI antenna system [54]. Such interpretation may be supported by the recent results of Drop and co-workers, who showed that Lhca2 and Lhca9, two algal LHCI monomers present in the PSI–LHCI complex in the 1:1 ratio with the core, are only loosely associated with it [7]. Melkozernov and co-workers also found that in the kinetic data obtained at 77 K the slow ~100-ps excitation equilibration phase is not observed and stated that at low temperatures the LHCI antenna system is energetically uncoupled from the PSI core [57]. In turn, Ihalainen and co-workers suggested that the long-lived phase cannot be due to "slow" energy transfer, and they assigned it to an unrelaxed state of the pigment–protein complex that, on this time-scale, is converted into the final emitting state [56].

Generally, a weak binding between different antenna peptides does not imply a slow energy transfer between them. However, in some recent experiments for PSII supercomplexes, such slow excitation energy transfer between extra LHCII trimers and $C_2S_2M_2$ form of PSII was postulated [58]. Under low- to medium-light growth conditions, the thylakoid membrane contains up to four more LHCII trimers per dimeric PSII as compared to the $C_2S_2M_2$ complex and then the average PSII lifetime is ~330 ps [59], more than double the value found for $C_2S_2M_2$ [58]. It was also calculated, using a coarse-grained model, that the hopping time from the extra LHCII trimers to the $C_2S_2M_2$ complex is 10–20 times slower than for the internal LHCII trimers [58]. However, it should also be noted that these extra LHCII trimers cannot be purified together with the PSII and that their position and organization is still questioned. In the case of Lhca2 and Lhca9, the situation is different because they can be isolated together with the whole PSI–LHCI complex.

In the case of our whole cell (in vivo) measurements, the situation is different from the case of isolated complexes. The third component is now characterized by a decay time of ~170 ps, which is shorter compared to that observed in both preparations of isolated complexes (PSI core and PSI–LHCI) and it is not accompanied by the nanosecond component. Moreover, the value of its decay time (~170 ps) is low enough to be fitted accurately in the analyzed time window, hence the effect of decay time truncation can be excluded in this case (see the Results section). All these observations suggest that the long-lived fluorescence signal does not come from the LHCI peptides dissociated from intact PSI–LHCI complexes. It could be assigned to the slow energy transfer between some loosely attached LHCI monomers and the rest of the antenna system. Such possibility has been already discussed above for the isolated complexes. However, another interpretation of this 170-ps phase is also possible. The CC2696 strain of *C. reinhardtii* investigated here lacks PSII core and most of LHCII (see the Materials and methods section). However, some LHCII can be still present in the cells of this mutant. Thus, once again we need to consider two possibilities: (1) LHCII trimers are attached to the antenna PSI–LHCI complexes or (2) free LHCII trimers, not attached to the PSI–LHCI complexes, are present in the thylakoid membranes of the CC2696 cells.

Excitation energy transfer in the isolated plant PSI–LHCI–LHCII complexes has been already investigated [60]. It was shown that attachment of LHCII trimer to the PSI–LHCI complex results in a moderate increases of 40- and 100-ps components' amplitudes in the 670- to 690-nm interval, where the LHCII decay occurs. Obviously, this leads to an increase of the average excitation lifetime in this spectral region from 42 ps in the PSI–LHCI to 60 ps in PSI–LHCI–LHCII. We can imagine that a similar effect could be observed when LHCII trimers would be attached to the algal PSI–LHCI complex.

The excitation decay in free plant LHCII trimers was also studied in the past [61] and nearly monoexponential decay with lifetime of ~3.8 ns (86%) was observed. A small fraction of the trimers (11%) showed a shorter decay time (1.96 ns). Both decay times observed for free trimeric LHCII are much longer than the long-lived component found in our whole cells. However, upon aggregation of LHCII trimers, the fluorescence decay becomes considerably faster and can be described by three major components with decay times of 33 ps (34%), 180 ps (43%) and 0.5 ns (20%) or the average lifetime of ~190 ps [61]. Lifetime of the second dominating component and the average excitation lifetime observed for trimeric LHCII aggregates have values very close to the decay time of the third extra component detected in our whole cell measurements.

In summary, in the whole cells, the ~170-ps phase may originate from the slow excitation transfer between some weakly bound LHCI monomers or LHCII trimers and the rest of the PSI–LHCI antenna system or may reflect excitation decay in the LHCII aggregates due to aggregation-induced quenching. None of these possibilities can be excluded based on our measurements and discussed literature.

4.3. Overall fluorescence decay in PSI and PSI–LHCI

To obtain one numerical parameter describing the excitation dynamics, we calculated the average decay time for all investigated systems on the basis of the TR1/2/3 results (Table 1). As we discussed above, the exact origin of the third "extra" phase (decay times of 160–310 ps) remains unclear. When this component represents excitation decay in the free LHCI monomers (in isolated complexes or whole cells) or free LHCII trimers (in whole cells), it should be excluded from the calculations. When it is assigned to slow excitation transfer from weakly bound LHCI monomers (in isolated complexes or whole cells) or from LHCII trimers (in whole cells), then it should be included in the calculation, if we only want to obtain parameter describing the excitation decay in the whole existing complex of PSI–LHCI (in isolated complexes or whole cells) or PSI–LHCI–LHCII (in whole cells). Therefore, we decided to perform the calculations in two different ways, i.e. taking this component into account ($\langle\tau_{123}\rangle$) or excluding it ($\langle\tau_{12}\rangle$). The longest, blue-shifted component (decay times of 3.5–5 ns), observed for isolated complexes, was generally assigned to uncoupled chlorophylls, but partially it may also reflect fluorescence decay in free LHCI monomers. Therefore it was not included in our calculations. In the case of whole cells, such nanosecond component is simply not observed. Some interesting observations can be made for the average decay times calculated only for the two fastest components ($\langle\tau_{12}\rangle$ in Table 1):

1) The average decay time ($\langle\tau_{12}\rangle$) of the PSI in the whole cells is similar to that in the isolated PSI–LHCI complexes.
2) The difference in average decay time between systems with open and closed RCs is equal to ~4 ps, both in the case of PSI core and PSI–LHCI complexes.
3) The average decay time in the case of PSI–LHCI complexes (both isolated and in whole cells) is about 7 ps longer than in the PSI core, in open as well as in closed states.

4.4. Lifetime of the excited state in LHCI

We next wished to calculate the average lifetime of the excited state created by photon absorption in LHCI antenna $\langle\tau_{12}\rangle^{LHCI}$. To do this, we had to make an assumption about the number of chlorophylls *a* forming the antenna system in the PSI core and LHCI moiety (using 400-nm laser pulses we preferentially excited chlorophyll *a*). According to the data presented by authors of isolation and purification methods [26,27], the total number of chlorophyll *a* molecules in our PSI–LHCI preparation should be twice as large as in the PSI core preparation (see the Material and methods section). However, because the precise ratio of

Table 2
The average decay time of the excited state created by photon absorption in LHCI antenna $\langle\tau_{12}\rangle^{LHCI}$, calculated according to Eq. (5) and on the basis of the average decay times $\langle\tau_{12}\rangle$ presented in Table 1.

Initial excitation distribution [%]	PSI core		65	60	55	50	45	40	35
	LHCI		35	40	45	50	55	60	65
$\langle\tau_{12}\rangle^{LHCI}$ [ps]	PSI–LHCI	Open RC	32.4	30.1	28.2	26.8	25.6	24.6	23.8
		Closed RC	37.1	34.7	32.7	31.2	29.9	28.9	28.0
	Whole cells		34.5	32.4	30.7	29.4	28.3	27.4	26.6
$\langle\tau_{12}\rangle^{LHCI} - \langle\tau_{12}\rangle^{PSI\ core}$ [ps]	PSI–LHCI	Open RC	18.6	16.3	14.4	13.0	11.8	10.8	10.0
		Closed RC	19.7	17.3	15.3	13.8	12.5	11.5	10.6
	Whole cells		18.5	16.2	14.4	12.9	11.8	10.8	9.9

Calculations were performed for a wide range of possible initial excitation distributions between the PSI core and LHCI antenna system. See text for more details.

chlorophylls in the PSI core and LHCI system is not known, we decided to extend our calculation to a wider range of possible initial excitation distributions between these two compartments (see Table 2). Excitation distributed in 35% in the core and in 65% in the LHCI antenna system may reflect the situation, when the core contains about 90 chlorophylls *a* whereas LHCI system is composed of about 165 chlorophylls *a*. In turn, the initial excitation of the core in 65% and the LHCI antenna system in 35% would be observed if the LHCI system contained only 50 chlorophylls *a*.

The total average decay time for the PSI–LHCI complexes can be generally expressed by the equation:

$$\langle\tau_{12}\rangle^{PSI-LHCI} = a\langle\tau_{12}\rangle^{PSI\ core} + b\langle\tau_{12}\rangle^{LHCI}, \quad (5)$$

where *a* and *b* represent the percentage distribution of the initial excitation over the PSI core and LHCI antenna system, respectively. The $\langle\tau_{12}\rangle^{PSI-LHCI}$ and $\langle\tau_{12}\rangle^{PSI\ core}$ are the average decay times calculated based on the two fastest components for the PSI–LHCI complexes and PSI core, respectively (shown in Table 1). This means that possible slow excitation transfer from weakly bound LHCI monomers (in isolated complexes or whole cells) or from LHCII trimers (in whole cells) is not included in this calculation. The $\langle\tau_{12}\rangle^{LHCI}$ values thus calculated are presented in Table 2 and indicate that the trapping time of excitations created in the well coupled LHCI antenna system may be about 10–20 ps longer than excitations created in the PSI core antenna. However, for the most probable initial excitation distribution, i.e. ratios between 45/55 and 55/45, this time is in the range of 12–15 ps. For comparison, it was earlier found for plant PSI–LHCI crystals that the average excited state lifetime is 10 ± 5 ps longer when LHCI is excited than when the PSI core is excited [62].

4.5. Algal PSI vs. plant PSI

Excitation dynamics in plant PSI was intensively investigated over the past several years by time-resolved fluorescence measurements using TCSPS (time correlated single photon counting) [32,35,55,63,64] or streak camera [21,55]. Studies were performed for PSI core preparations [32,35] as well as for PSI–LHCI complexes [21,32,35,55,63,64]. Our results for algal PSI will be compared here in detail only with the plant PSI data obtained by the streak camera measurements. Fluorescence decays obtained in those studies, both for PSI core [55] and PSI–LHCI [21,55], were described by three main components with decay times of 3–5 ps, 18–20 ps and 63–82 ps, which are generally shorter than the decay times of analogous components obtained by us for algal PSI. However, while comparing, we should keep in mind that plant PSI data were obtained only for short time windows, i.e. ~160 ps (TR1) [55] or ~200 ps (TR1) and 550–800 ps (TR2) [21].

The DAS associated with the shortest decay time (3–5 ps) obtained for plant PSI core and PSI–LHCI was mainly conservative, with a positive contribution around ~680 nm and a negative one around ~720 nm, and was assigned to the excitation energy equilibration between bulk and long-wavelength chlorophylls. Its conservative shape suggests that hardly any trapping takes place in plant PSI particles on this time scale. In the case of our algal PSI studies, purely conservative DAS was observed only for PSI–LHCI with closed RC measured in TR1/2 (Fig. 2E) as well as for PSI–LHCI with open RC measured in TR1 and analyzed simultaneously with PSI core data (Fig. 3B). The decay time associated with this DAS was equal to ~6 ps. However, it should be noted here, that in the case of algal PSI particles (both PSI core and PSI–LHCI) with open RC (Fig. 1A–C, 2A–C), not much longer decay times (6.5–8.5 ps) primarily describe excitation trapping. This apparent difference may be due to the fact that excitation energy transfer to long-wavelength chlorophylls in plant PSI is more efficient compared to algal PSI. Consequently, it dominates the shortest component observed for plant PSI and strongly influences its decay time.

It was shown that excitations produced in plant PSI core decay mainly with an 18-ps lifetime (redox state of RC was not chemically controlled) [55]. This value agrees well with the overall average trapping time estimated by us for algal PSI core with closed RC ($\langle\tau_{12}\rangle$ = 17.4 ps), based on the two fastest components dominating the overall fluorescence decay (~90%). A small contribution of a 63-ps component with red emission was also observed in plant PSI core [55]. It was assigned to the presence of long-wavelength chlorophylls in the core. However, this long-lived signal may also come from a trace amount of LHCI contaminating the sample, but this possibility was neglected in the cited work [55]. The average trapping time calculated for plant PSI core with the inclusion of a 63-ps component was equal to ~23 ps.

In the case of plant PSI–LHCI, contributions of both trapping components (decay times of 18–20 ps and 63–82 ps) to the overall fluorescence decay are almost equal, but they differ spectrally [21,55]. DAS of the shorter component has one maximum at ~685 nm and long-wavelength tail, similar to that observed by us for algal PSI–LHCI complexes. DAS of the longer component is composed of two bands with maxima at ~685 nm and ~725 nm. However, the long-wavelength band clearly dominates in that DAS. Comparison of the trapping components obtained for plant PSI core and plant PSI–LHCI complexes leads to the conclusion that long-wavelength chlorophylls in plant PSI complexes are located mostly in the LHCI antenna system, that we observed also for algal PSI. However, they are more red-shifted (with respect to bulk chlorophylls) compared to the algal PSI. There is also a general agreement that the slow excitation decay, reflected in plant PSI–LHCI by the slower trapping component (decay time of 63–82 ps), is caused by the need for uphill excitation energy transfer from the low energy states before a trapping. The analogous component, fitted by us for isolated algal PSI–LHCI complexes in TR1/2, is characterized by decay time similar to that found for plant PSI–LHCI, but when the fitting is performed for the longer time window (TR1/2/3), the obtained decay time is much longer (270–310 ps). Moreover, in the case of algal PSI–LHCI, the DAS of this component is not red-shifted compared to the shorter component (decay time of 28–31 ps), but its long-wavelength tail is even less pronounced. This suggests that the origin of long-lived component in algal PSI–LHCI must be different than in plant PSI–LHCI. We discussed this issue more broadly in the Origin of the slow fluorescence decay section. The average trapping time calculated for plant PSI–LHCI is equal to ~48 ps [21,55]. If we assume, that long-lived component in our algal PSI preparations describes the free LHCI or

LHCII, then the average lifetime calculated based only on the two fastest components is correct, and its value ($\langle\tau_{12}\rangle = 20$–$24$ ps, Table 1) is two times smaller than that found for plant PSI–LHCI. This would support previous hypothesis that the amount and energies of long-wavelength chlorophylls have larger effect on the average trapping time in PSI–LHCI complexes than the antenna size [21], because the LHCI antenna system in algal PSI is bigger (9–14 LHCI monomers) than in plant PSI (4 LHCI monomers). If the long-lived component found for algal PSI–LHCI describes the LHCI monomers weakly bound to the complex, it should be included in the calculation of the average decay time ($\langle\tau_{123}\rangle$, Table 1). It would then have a value of 38–52 ps (Table 1), which would be comparable with that found for plant PSI–LHCI.

5. Conclusions

The most important achievements and findings, reflecting the scientific novelty of our work, are as follows:

1) Our article shows for the first time the time-resolved fluorescence data obtained by the same experimental technique and under the same experimental conditions for three different PSI preparations: isolated PSI cores, isolated PSI–LHCI complexes and PSI complexes in the whole living cells. This allows a direct comparison of results obtained for these three PSI preparations. Such regular comparative studies have never been done before.
2) We made an effort to perform the global analysis and present its results for different experimental time windows, that has never been done before for the fluorescence time-resolved data obtained for PSI preparations. This novel way of presenting time-resolved results is extremely important for two reasons: (A) It allows comparing our results with the literature data obtained in many different time windows. (B) It shows that analysis of data obtained in different time windows may give different results (lifetimes and amplitudes) and unreasonably lead to different conclusions. Our approach illustrates that such results are still consistent with each other, if we only take into account the limitations of global analysis.
3) We found that average decay time for algal PSI core with RC in open and closed states is equal to 13.8 ps and 17.4 ps, respectively. The latter value is comparable with the streak camera data obtained previously for plant PSI core [55].
4) The most essential difference with respect to the previous works on algal PSI core refers to the two issues of fundamental importance: total rate of excitation decay in the antenna system of algal PSI core and fluorescence spectrum of the excited reaction center (RC^*). We addressed our comparison to probably the most relevant work in this topic published by Holzwarth and co-workers [19] and we found that: (A) the overall excitation decay in the PSI core is faster in the case of our preparation than in the case of the preparation analyzed by Holzwarth and co-workers, that suggests, together with other observations, contamination of their preparation by LHCI (at least stronger than in our study), (B) the long-wavelength fluorescence observed by Holzwarth and co-workers for their PSI core preparation and assigned by them exclusively to the reaction center excited state may also originate from the long-wavelength chlorophylls located in the LHCI antennas, as suggested by our measurements. Thus, very detailed modeling performed by Holzwarth and co-workers based on their experimental data and conclusions resulting from it may not be fully correct.
5) According to our measurements, the excitation energy equilibration between bulk and long-wavelength chlorophylls in algal PSI–LHCI complexes occurs with a ~6-ps lifetime and most of the excited states of the long-wavelength chlorophylls decay with a lifetime of ~30 ps. The average decay time in the algal PSI–LHCI complexes depends on the interpretation of the long-lived component (decay time of 160–310 ps) and may vary from 20 to 52 ps. These values are similar or shorter than that found previously for plant PSI–LHCI complexes (~48 ps). This may support the hypothesis that the amount and energies of long-wavelength chlorophylls have a larger effect on the average trapping time in PSI–LHCI complexes than the antenna size [21].
6) Fluorescence decay in PSI–LHCI complexes working in vivo, i.e. embedded in the thylakoid membrane in whole living cells, was for the first time measured with a high temporal resolution (~3.5 ps). Such previous studies were done a long time ago and with extremely low temporal resolution, i.e. with the instrument response function (IRF) of 50–70 ps (FWHM) [22,23]. We have demonstrated that excitation dynamics in PSI–LHCI complexes in vivo is almost identical to that observed in vitro for isolated complexes, with the exception of processes occurring on long time scales (decay times of 160–310 ps and 3.5–5 ns).
7) The long lived components found both in algal PSI preparations (decay times of ~160–310 ps) and reported in the literature for plant PSI (decay times of ~60–80 ps) have different spectral properties. In plant PSI, this component's DAS is red-shifted and can be assigned to slow uphill excitation energy transfer from long-wavelength chlorophylls. In the case of our algal PSI preparations, analogous DAS is not red-shifted at all, thus the long decay time of this component may result from some structural arrangements. In the case of whole cells, where LHCI dissociation due to isolation procedure can be excluded, this structural effect must have a natural origin: either (A) weak coupling of some LHCI monomers to the complex, or (B) presence of LHCII trimers attached to the complex, or (C) presence of free LHCII trimers in the thylakoid membranes.
8) Two more interesting observations were done based on average decay time values, calculated excluding free LHCI monomers or LHCI monomers weakly bound to the complex: (A) closing of RC leads to elongation of average decay time of about 4 ps, both in PSI core and PSI–LHCI complexes (B) the average decay time of excitations created in the LHCI antenna system, is about 12–15 ps longer than the decay time of excitations created in the PSI core antenna.

Acknowledgements

The research leading to these results has received funding from LASERLAB-EUROPE II: grant agreement no. 228334. K.G. gratefully acknowledges financial support from the Polish government (scientific project no. N N202 085440). K.R. gratefully acknowledges support from the U.S. National Science Foundation (grant MCB-1052573). J.S. acknowledges support from BioSolar Cells, cofinanced by the Dutch Ministry of Economic Affairs, Agriculture and Innovation. W.G. is a scholarship holder within the project "Integrated program supporting the development of the Adam Mickiewicz University in Poznan in the field of physical sciences: Pro-innovative education, competent staff, graduates of the future" (POKL.04.01.01-00-133/09-00, Sub-measure 4.1.1 of the Human Capital Operational Programme, co-financed by European Union under the European Social Fund).

References

[1] R.E. Blankenship, Molecular Mechanisms of Photosynthesis, Blackwell Science Ltd., 2002
[2] H.V. Scheller, P.E. Jensen, A. Haldrup, C. Lunde, J. Knoetzel, Role of subunits in eukaryotic Photosystem I, Biochim. Biophys. Acta 1507 (2001) 41–60.
[3] A. Ben-Shem, F. Frolow, N. Nelson, Crystal structure of plant photosystem I, Nature 426 (2003) 630–635.
[4] A. Amunts, O. Drory, N. Nelson, The structure of a plant photosystem I supercomplex at 3.4 Å resolution, Nature 447 (2007) 58–63.
[5] M. Germano, A.E. Yakushevska, W. Keegstra, H.J. van Gorkom, J. Dekker, E.J. Boekema, Supramolecular organization of photosystem I and light harvesting complex I in *Chlamydomonas reinhardtii*, FEBS Lett. 525 (2002) 121–125.
[6] J. Kargul, J. Nield, J. Barber, Three-dimensional reconstruction of a light-harvesting complex I–photosystem I (LHCI–PSI) supercomplex from the green alga *Chlamydomonas reinhardtii* — insights into light harvesting for PSI, J. Biol. Chem. 278 (2003) 16135–16141.
[7] B. Drop, M. Webber-Birungi, F. Fusetti, R. Kouřil, K.E. Redding, E.J. Boekema, R. Croce, Photosystem I of *Chlamydomonas reinhardtii* contains nine light-harvesting

complexes (Lhca) located on one side of the core, J. Biol. Chem. 286 (2011) 44878–44887.
[8] A. Haldrup, P.E. Jensen, H.V. Scheller, The low molecular mass subunits in higher plant photosystem I, in: J.H. Golbeck (Ed.), Photosystem I. The light-driven plastocyanin:ferredoxin oxidoreductase, Advances in Photosynthesis and Respiration, vol. 24, Springer, Dordrecht, 2006, pp. 139–154.
[9] P. Jensen, A. Haldrup, S. Zhang, Molecular dissection of photosystem I in higher plants: topology, structure and function, Physiol. Plant. 119 (2003) 313–321.
[10] P. Jordan, P. Fromme, H. Witt, O. Klukas, W. Saenger, N. Krauss, Three-dimensional structure of cyanobacterial photosystem I at 2.5 Å resolution, Nature 411 (2001) 909–919.
[11] K. Redding, A. van der Est, The directionality of electron transfer in photosystem I, in: J.H. Golbeck (Ed.), Photosystem I. The light-driven plastocyanin:ferredoxin oxidoreductase, Advances in Photosynthesis and Respiration, vol. 24, Springer, Dordrecht, 2006, pp. 413–437.
[12] M. Guergova-Kuras, B. Boudreaux, A. Joliot, P. Joliot, K. Redding, Evidence for two active branches for electron transfer in photosystem I, Proc. Natl. Acad. Sci. U. S. A. 98 (2001) 4437–4442.
[13] V.M. Ramesh, K. Gibasiewicz, S. Lin, S.E. Bingham, A.N. Webber, Bidirectional electron transfer in photosystem I: accumulation of A_0^- in A-side or B-side mutants of the axial ligand to chlorophyll A_0, Biochemistry 43 (2004) 1369–1375.
[14] V.M. Ramesh, K. Gibasiewicz, S. Lin, S.E. Bingham, A.N. Webber, Replacement of the methionine axial ligand to the primary electron acceptor A_0 slows the A_0^- reoxidation dynamics in Photosystem I, Biochim. Biophys. Acta 1767 (2007) 151–160.
[15] Y. Li, A. van der Est, M.G. Lucas, V.M. Ramesh, F. Gu, A. Petrenko, S. Lin, A.N. Webber, F. Rappaport, K. Redding, Directing electron transfer within Photosystem I by breaking H-bonds in the cofactor branches, Proc. Natl. Acad. Sci. U. S. A. 103 (2006) 2144–2149.
[16] W. Giera, K. Gibasiewicz, V.M. Ramesh, S. Lin, Electron transfer from A_0 to A_1 in Photosystem I from *Chlamydomonas reinhardtii* occurs in both the A and B branch with 25–30-ps lifetime, Phys. Chem. Chem. Phys. 11 (2009) 5186–5191.
[17] M.G. Müller, C. Slavov, R. Luthra, K.E. Redding, A.R. Holzwarth, Independent initiation of primary electron transfer in the two branches of the photosystem I reaction center, Proc. Natl. Acad. Sci. U. S. A. 107 (2010) 4123–4128.
[18] M.G. Müller, J. Niklas, W. Lubitz, A.R. Holzwarth, Ultrafast transient absorption studies on Photosystem I reaction centers from *Chlamydomonas reinhardtii*. 1. A new interpretation of the energy trapping and early electron transfer steps in Photosystem I, Biophys. J. 85 (2003) 3899–3922.
[19] A.R. Holzwarth, M.G. Müller, J. Niklas, W. Lubitz, Charge recombination fluorescence in photosystem I reaction centers from *Chlamydomonas reinhardtii*, J. Phys. Chem. B 109 (2005) 5903–5911.
[20] W. Giera, V.M. Ramesh, A.N. Webber, I. van Stokkum, R. van Grondelle, K. Gibasiewicz, Effect of the P700 pre-oxidation and point mutations near A_0 on the reversibility of the primary charge separation in Photosystem I from *Chlamydomonas reinhardtii*, Biochim. Biophys. Acta Bioenerg. 1797 (2010) 106–112.
[21] J.A. Ihalainen, I.H.M. van Stokkum, K. Gibasiewicz, M. Germano, R. van Grondelle, J.P. Dekker, Kinetics of excitation trapping in intact Photosystem I of *Chlamydomonas reinhardtii* and *Arabidopsis thaliana*, Biochim. Biophys. Acta 1706 (2005) 267–275.
[22] T.G. Owens, S.P. Webb, L. Mets, R.S. Alberte, G.R. Fleming, Antenna structure and excitation dynamics in photosystem I. Studies with mutants of *Chlamydomonas reinhardtii* lacking photosystem II, Biophys. J. 56 (1989) 95–106.
[23] M. Werst, Y. Jia, L. Mets, G.R. Fleming, Energy transfer and trapping in the photosystem I core antenna. A temperature study, Biophys. J. 61 (1992) 868–878.
[24] H. Lee, S.E. Bingham, A.N. Webber, Specific mutagenesis of reaction center proteins by chloroplast transformation of *Chlamydomonas*, in: L. McIntosh (Ed.), Methods in Enzymology, vol. 297, Academic Press, Boca Raton, FL, 1998, pp. 311–319.
[25] N.H. Chua, P. Bennoun, Thylakoid membrane polypeptides of *Chlamydomonas reinhardtii*: wild-type and mutant strains deficient in photosystem II reaction center, Proc. Natl. Acad. Sci. U. S. A. 72 (1975) 2175–2179.
[26] V.M. Ramesh, A.N. Webber, Rapid isolation and purification of photosystem I chlorophyll-binding protein from *Chlamydomonas reinhardtii*, in: R. Carpentier (Ed.), Methods in Molecular Biology, vol. 274, Humana Press Inc., New York, 2004, pp. 19–28.
[27] G. Gulis, V.K. Narasimhulu, L.N. Fox, K.E. Redding, Purification of His6-tagged Photosystem I from *Chlamydomonas reinhardtii*, Photosynth. Res. 96 (2008) 51–60.
[28] E.H. Harris, The *Chlamydomonas* Sourcebook. A Comprehensive Guide to Biology and Laboratory Use, Academic Press, San Diego, 1989.
[29] N. Fischer, P. Setif, J.D. Rochaix, Targeted mutations in the psaC gene of *Chlamydomonas reinhardtii*: preferential reduction of F_B at low temperature is not accompanied by altered electron flow from photosystem I to ferredoxin, Biochemistry 36 (1997) 93–102.
[30] B. Gobets, I.H.M. van Stokkum, M. Rogner, J. Kruip, E. Schlodder, N.V. Karapetyan, J.P. Dekker, R. van Grondelle, Time-resolved fluorescence emission measurements of photosystem I particles of various cyanobacteria: a unified compartmental model, Biophys. J. 81 (2001) 407–424.
[31] S. Turconi, G. Schweitzer, A.R. Holzwarth, Temperature-dependence of picosecond fluorescence kinetics of a cyanobacterial photosystem-I particle, Photochem. Photobiol. 57 (1993) 113–119.
[32] E. Engelmann, G. Zucchelli, A.P. Casazza, D. Brogioli, F.M. Garlaschi, R.C. Jennings, Influence of the photosystem I–light harvesting complex I antenna domains on fluorescence decay, Biochemistry 45 (2006) 6947–6955.
[33] N.V. Karapetyan, D. Dorra, G. Schweitzer, I.N. Bezsmertnaya, A.R. Holzwarth, Fluorescence spectroscopy of the longwave chlorophylls in trimeric and monomeric photosystem I core complexes from the cyanobacterium *Spirulina platensis*, Biochemistry 36 (1997) 13830–13837.
[34] A.M. Nuijs, V.A. Shuvalov, H.J. van Gorkom, J.J. Plijter, L.N.M. Duysens, Picosecond absorbance difference spectroscopy on the primary reactions and the antenna excited states in photosystem I particles, Biochim. Biophys. Acta 850 (1986) 310–318.
[35] C. Slavov, M. Ballottari, T. Morosinotto, R. Bassi, A.R. Holzwarth, Trap-limited charge separation kinetics in higher plant photosystem i complexes, Biophys. J. 94 (2008) 3601–3612.
[36] M. Byrdin, I. Rimke, E. Schlodder, D. Stehlik, T.A. Roelofs, Decay kinetics and quantum yields of fluorescence in photosystem I from *Synechococcus elongatus* with P700 in the reduced and oxidized state: are the kinetics of excited state decay trap-limited or transfer-limited? Biophys. J. 79 (2000) 992–1007.
[37] R. Blankenship, A. McGuire, K. Sauer, Chemically induced dynamic electron polarization in chloroplasts at room temperature: evidence for triplet state participation in photosynthesis, Proc. Natl. Acad. Sci. U. S. A. 72 (1975) 4943–4947.
[38] M.C.W. Evans, C.K. Sihra, A.R. Slabas, The oxidation–reduction potential of the reaction-centre chlorophyll (P700) in photosystem I, Biochem. J. 162 (1977) 75–85.
[39] S. Krawczyk, W. Maksymiec, Stark effect in P700, the primary electron donor of Photosystem I, FEBS Lett. 286 (1991) 110–112.
[40] E. Schlodder, F. Lendzian, J. Meyer, M. Çetin, M. Brecht, T. Renger, N.V. Karapetyan, Long-wavelength limit of photochemical energy conversion in photosystem i, J. Am. Chem. Soc. 136 (2014) 3904–3918.
[41] J.J. Snellenburg, S. Laptenok, R. Seger, K.M. Mullen, I.H.M. van Stokkum, Glotaran: a Java-based graphical user interface for the R-package TIMP, J. Stat. Softw. 49 (2012) 1–22.
[42] A.R. Holzwarth, Data analysis of time-resolved measurements, in: J. Amesz, A.J. Hoff (Eds.), Biophysical techniques in photosynthesis, Advances in Photosynthesis and Respiration, vol. 3, Kluwer Academic Publishers, Dordrecht, 1996, pp. 75–92.
[43] H. van Amerongen, R. van Grondelle, L. Valkunas, Photosynthetic Excitons, World Scientific, London, 2000.
[44] I.H.M. van Stokkum, T.E. Desquilbet, C.D. van der Weij-de Wit, J.J. Snellenburg, R. van Grondelle, J.C. Thomas, J.P. Dekker, B. Robert, Energy transfer and trapping in red-chlorophyll-free photosystem I from *Synechococcus* WH 7803, J. Phys. Chem. B 117 (2013) 11176–11183.
[45] S. Santabarbara, K.E. Redding, F. Rappaport, Temperature dependence of the reduction of $P700^+$ by tightly bound plastocyanin in vivo, Biochemistry 48 (2009) 10457–10466.
[46] F. Drepper, M. Hippler, W. Nitschke, W. Haehnel, Binding dynamics and electron transfer between plastocyanin and photosystem I, Biochemistry 35 (1996) 1282–1295.
[47] A.B. Hope, Electron transfers amongst cytochrome f, plastocyanin and photosystem I: kinetics and mechanisms, Biochim. Biophys. Acta 1456 (2000) 5–26.
[48] V.M. Ramesh, M. Guergova-Kuras, P. Joliot, A.N. Webber, Electron transfer from plastocyanin to the photosystem I reaction center in mutants with increased potential of the primary donor in *Chlamydomonas reinhardtii*, Biochemistry 41 (2002) 14652–14658.
[49] K. Gibasiewicz, A. Szrajner, J.A. Ihalainen, M. Germano, J.P. Dekker, R. van Grondelle, Characterization of low-energy chlorophylls in the PSI–LHCI supercomplex from *Chlamydomonas reinhardtii*. A site-selective fluorescence study, J. Phys. Chem. B 109 (2005) 21180–21186.
[50] M. Mozzo, M. Mantelli, F. Passarini, S. Caffarri, R. Croce, R. Bassi, Functional analysis of Photosystem I light-harvesting complexes (Lhca) gene products of *Chlamydomonas reinhardtii*, Biochim. Biophys. Acta 1797 (2010) 212–221.
[51] K. Gibasiewicz, V.M. Ramesh, A.N. Melkozernov, S. Lin, N.W. Woodbury, R.E. Blankenship, A.N. Webber, Excitation dynamics in the core antenna of PS I from *Chlamydomonas reinhardtii* CC 2696 at room temperature, J. Phys. Chem. B 105 (2001) 11498–11506.
[52] K. Gibasiewicz, V.M. Ramesh, S. Lin, K. Redding, N.W. Woodbury, A.N. Webber, Excitonic interactions in wild-type and mutant PSI reaction centers, Biophys. J. 85 (2003) 2547–2559.
[53] Y. Jia, J.M. Jean, M.M. Werst, C.-K. Chan, G.R. Fleming, Simulations of the temperature dependence of energy transfer in the PSI core antenna, Biophys. J. 63 (1992) 259–273.
[54] A.N. Melkozernov, J. Kargul, S. Lin, J. Barber, R.E. Blankenship, Energy coupling in the PSI–LHCI supercomplex from the green alga *Chlamydomonas reinhardtii*, J. Phys. Chem. B 108 (2004) 10547–10555.
[55] E. Wientjes, I.H.M. van Stokkum, H. van Amerongen, R. Croce, The role of the individual Lhcas in photosystem I excitation energy trapping, Biophys. J. 101 (2011) 745–754.
[56] J.A. Ihalainen, R. Croce, T. Morosinotto, I.H.M. van Stokkum, R. Bassi, J.P. Dekker, R. van Grondelle, Excitation decay pathways of Lhca proteins: a time-resolved fluorescence study, J. Phys. Chem. B 109 (2005) 21150–21158.
[57] A.N. Melkozernov, J. Kargul, S. Lin, J. Barber, R.E. Blankenship, Spectral and kinetic analysis of the energy coupling in the PS I–LHC I supercomplex from the green alga *Chlamydomonas reinhardtii* at 77 K, Photosynth. Res. 86 (2005) 203–215.
[58] S. Caffarri, K. Broess, R. Croce, H. van Amerongen, Excitation energy transfer and trapping in higher plant photosystem II complexes with different antenna sizes, Biophys. J. 100 (2011) 2094–2103.
[59] B. van Oort, M. Alberts, H. van Amerongen, Effect of antenna-depletion in Photosystem II on excitation energy transfer in *Arabidopsis thaliana*, Biophys. J. 98 (2010) 922–931.
[60] P. Galka, S. Santabarbara, Thi Thu Huong Khuong, H. Degand, P. Morsomme, R.C. Jennings, E.J. Boekema, S. Caffarri, Functional analyses of the plant photosystem I–light-harvesting complex II supercomplex reveal that light-harvesting complex II loosely bound to photosystem II is a very efficient antenna for photosystem I in state II, Plant Cell 24 (2012) 2963–2978.

[61] B. van Oort, A. van Hoek, A.V. Ruban, H. van Amerongen, Aggregation of light-harvesting complex II leads to formation of efficient excitation energy traps in monomeric and trimeric complexes, FEBS Lett. 581 (2007) 3528–3532.
[62] B. van Oort, A. Amunts, J.W. Borst, A. van Hoek, N. Nelson, H. van Amerongen, R. Croce, Picosecond fluorescence of intact and dissolved PSI–LHCI crystals, Biophys. J. 95 (2008) 5851–5861.
[63] R. Croce, D. Dorra, A.R. Holzwarth, R.C. Jennings, Fluorescence decay and spectral evolution in intact photosystem I of higher plants, Biochemistry 39 (2000) 6341–6348.
[64] R.C. Jennings, G. Zucchelli, S. Santabarbara, Photochemical trapping heterogeneity as a function of wavelength, in plant photosystem I (PSI–LHCI), Biochim. Biophys. Acta 1827 (2013) 779–785.